ingegneria sismica
International Journal of Earthquake Engineering
Anno XLII – Num.3 - 2025

# SEISMIC PERFORMANCE EVALUATION OF THE HISTORICAL YOZGAT CLOCK TOWER

*Ali Ekber Sever*[1,*], *Yakup Hakan Aydin*[2] *and Pinar Usta Evci*[1]

[1]Department of Civil Engineering, Isparta University of Applied Sciences, 32260 Isparta, Turkey

[2]Department of Mechanical Engineering, Isparta University of Applied Sciences, 32260 Isparta, Turkey

SUMMARY: *The seismic evaluation of historical masonry structures is very important for their preservation, particularly in seismic zones. An investigation of the dynamic performance and seismic sensitivity of the historical Yozgat Clock Tower in Turkey is presented in this paper. A three-dimensional finite element model of the historic tower is established in Abaqus, and the nonlinear performance of masonry is modeled utilizing the Concrete Damage Plasticity (CDP) material model. The performance assessment of the structure is performed through modal and nonlinear time-history analyses under appropriate ground-motion records. The fundamental natural frequency of the historic tower is found to be 5.64 Hz, which is in good agreement with those obtained from empirical expressions. It is found from nonlinear dynamic analyses that tensile, compressive, and plastic damage is mostly concentrated at the tower foundation level, while the above parts mostly behave like rigid bodies. This work emphasizes that the journal area is the critical area governing the seismic behavior of this tower and implies a future strategy for its restoration and strengthening.*

*KEYWORDS: Historical structures, dynamic behaviour, nonlinear time history analysis, modal analysis, concrete damaged plasticity*

## 1 Introduction

Historic masonry buildings, besides being significant examples of cultural heritage, have distinct architectural properties that can be studied from a structural standpoint. But such buildings are not designed by contemporary engineering concepts, and there may exist discontinuity, material degradation, or rigidity deficiency in such buildings. Such structures, especially in seismically active areas such as Turkey, can face severe damage in case of an earthquake. There is, therefore, an essential need to comprehend and investigate such seismic behavior. Among historic structures, it has been realized that masonry towers are especially prone to earthquakes [1, 2].

There are many studies in the literature that analyze the behavior of tower-type structures under earthquake effects. Kumar and Pallav [3] conducted seismic evaluation of a clock tower in India that showed severe cracks and material deterioration. They conducted static, modal,

*alisever@isparta.edu.tr
https://doi.org/10.65102/is202531

and time-history analyses and stated that, based on the critical areas, stress distributions show severe cracks and structural damage. Onat et al. studied the seismic performance of a masonry minaret [4]. They identified the damaged areas by nonlinear dynamic analyses and proposed appropriate retrofitting recommendations for the identified parts. Romero-Sánchez et al. studied the seismic behavior of the Giralda Tower in Spain [5]. Modal and nonlinear static analyses were performed on the structural model and stated that the maximum damage distribution was coherent with the results obtained from past earthquake records. Peña et al. studied the seismic behavior of a historic tower [6]. Nonlinear static (pushover) and dynamic analyses were applied to the structure, and it was specified that the base region is weaker under static and the top region under dynamic analysis. Çaktı et al. studied the seismic behavior of three historic minarets in Istanbul [7]. Nonlinear dynamic analyses were applied to determine the parts that each model will have damaged or collapsed. The authors have also compared the obtained results with the actual damage after past earthquakes.

Sánchez et al. assessed the seismic response of a historic masonry tower employing nonlinear analysis procedures [8]. In this research, the authors employed a three-dimensional numerical model and assessed the seismic response of the structure employing nonlinear time-history analyses. Based on the geometric and material characteristics of the structure, the authors identified tensile fractures and compressive crushing, especially at the top parts of the structure. Thus, the study demonstrated the efficiency of nonlinear analysis procedures for the seismic assessment of masonry buildings. Chisari et al. assessed the operational modal analysis and structural safety of a historic masonry bell tower [9]. In this research, the authors applied an operational modal analysis employing environmental vibration measurements and assessed the natural frequencies and modes of vibration for the structure. The validation of the numerical model was performed by comparing the obtained dynamic responses with those obtained employing the finite element model developed by the researcher. Additionally, the authors applied nonlinear analysis procedures for the assessment of the existing seismic response of the structure and identified vulnerable parts susceptible to seismic damage. Sánchez et al. assessed the role of soil-structure interaction on the seismic response of the historic Giralda Tower located at Seville [10]. The authors demonstrated the role of integrating soil-structure interaction on the model for evaluating the impact of neglecting soil-structure interaction on the vibration response and seismic response behavior of the structure. The study demonstrated seismic response behavior incongruities due to neglecting soil-structure interaction. Thus, the study underlined the prime significance of evaluating seismic response behavior employing the impact of soil-structure interaction for seismic analyses of historic masonry buildings.

Najafgholipour et al. investigated the dynamic behavior of old masonry towers under near- and far-fault ground motion and discussed the potential mechanisms of collapse [11]. The results indicated that the near-fault ground motion produced larger displacements, stress, and sudden damage to the towers. It was also identified in the far-fault records that the damage was more extensive and gradual. The authors pointed out that this issue was particularly important in high masonry towers with sensitive geometry and highlighted the importance of taking the ground motion type into account in seismic assessment. Cakiroglu et al. investigated the seismic behavior of a damaged masonry building prior to and after shotcrete application in the building damaged during the February 6, 2023, Kahramanmaraş earthquake [12]. The authors identified that shotcrete treatment enhanced shear resistance and energy dissipation. Uysal and Evci investigated the dynamic behavior of a registered masonry building and suggested proposals on the application of CFRP to improve the building [13]. The authors identified that the treatment with CFRP increased the tensile resistance of the structure and resisted the propagation of the

cracks.

Eight historical stone towers in Italy were investigated by authors Valente and Milani for seismic behavior when subjected to seismic forces, based on the investigation, the authors indicated that the geometric parameters of the tower, which influence the seismic behavior of the tower, are the thickness of the tower wall, the size of the tower, and the space inside the tower [14]. The seismic behavior of a masonry tower that was damaged during the 2012 Emilia earthquake was examined by authors Minghini et al., for which the authors used computer modeling for the tower, based on the results obtained, the authors indicated that both modal pushover analysis and response spectrum analysis methods are reliable for the determination of the seismic behavior of a masonry tower, based on the obtained results, the authors observed that the values obtained are accurate [15]. Acito et al. analyzed the collapse of a clock tower after the occurrence of an earthquake, based on which the authors indicated that the geometric parameters of the tower, along with the strength of the materials, influenced the collapse of the clock tower constructed using the strength of the chosen materials [16].

In addition to the aforementioned studies, a plethora of other researchers have conducted similar evaluations on the seismic behaviour of tower-type structures [17, 18, 19, 20, 21, 22, 23, 24, 25, 26, 27, 28].

## 1.1 Scope of the work

In this study, a comprehensive seismic assessment was conducted for the historical masonry Yozgat Clock Tower (see Figure 1) using nonlinear finite element modelling.

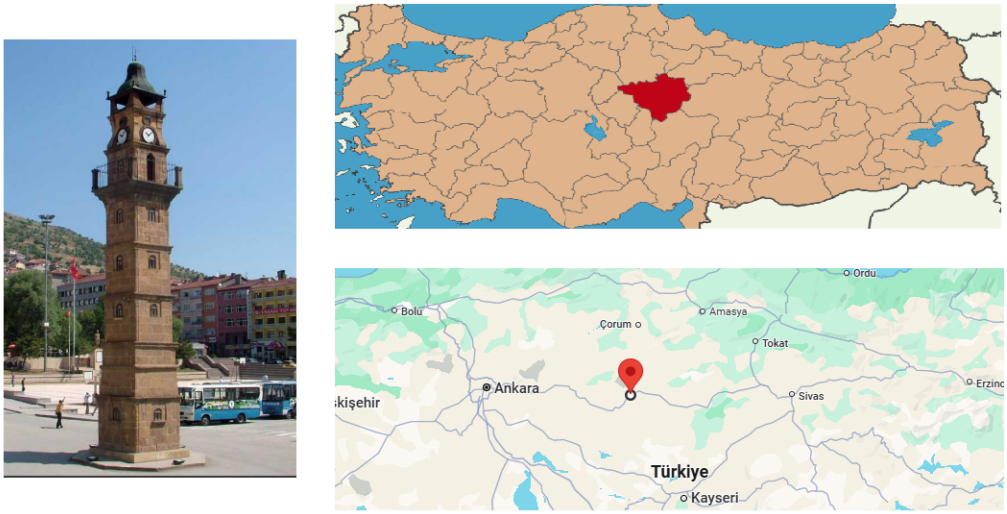


*Figure 1: Yozgat clock tower*

The primary objective of this study was to comprehend the seismic behaviour of the tower and to identify potential vulnerabilities in scenarios of strong ground motion. To this end, the structure was modelled in the ABAQUS finite element software, employing the Concrete Damaged Plasticity (CDP) model to capture the nonlinear material behaviour of masonry under cyclic loading. Time history analyses were conducted using representative ground motion records, and the structural response was evaluated in terms of stress concentrations and damage patterns. The primary contributions of this study are enumerated below. The nonlinear dynamic

behavior of the tower has been analyzed using nonlinear time history analyses with the parameters of the Concrete Damage Plastics (CDP) model, which enable the correct modeling of the phenomena of cracking and crushing of the masonry material.

The impact of finite element mesh size on the dynamic characteristics of the model has been studied, and there is an optimal mesh arrangement identified for efficient computation.

Damage-based performance assessment for the tower was done by correlating observed stress/strain concentrations to probable failure modes in an attempt to gain insights that could lead to the evolution of future retro-fitting or preservation approaches.

# 2 Materials and methods

## 2.1 Yozgat clock tower

The Yozgat clock tower is situated in the Cumhuriyet Square in the center of Yozgat. It is the only clock tower with historic importance inside the boundary of Yozgat. The clock tower was erected in 1908, consisting of seven levels, including the ground floor and the floor for the bells. The clock tower was made of cut stone, where each level is separated by a window installed in each facade. Inside, wooden stairs connect people to the upper levels. The top level is surrounded by a balcony, used as a balcony, topped with a bell. Below the bell, four clocks are installed in each façade [29]. The Yozgat clock tower's features and location are illustrated in Figure 1.

## 2.2 Modeling of the tower

In this investigation, a macromodeling approach based on the Finite Element Analysis framework has been employed. Macromodeling basically includes the modeling of the masonry material (stone as well as mortar) as a homogeneous composite material, whose spatial distribution is also modeled as that of the homogeneous composite material. The strength properties of the homogeneous composite wall are estimated using experimental studies or numerical homogenization techniques. Compared to the estimated results obtained using other modeling techniques, macromodeling has been quite comprehensive as well as effective, especially for the nonlinear analyses of the masonry arch bridges [30, 31]. The method has been widely employed for the assessment of masonry buildings [32, 33, 34].

A Finite Element Model of the historical Yozgat Clock Tower was prepared and analyzed for earthquake loading using finite elements. In determining the boundary conditions, it was hypothesised that all degrees of freedom at the base of the tower were fully constrained. Given the structure's fragile nature, a low damping ratio was assumed for seismic excitations, with a value of 5% adopted in the analyses.

A series of numerical simulations of the tower were conducted utilising the ABAQUS software programme. The geometric configuration of the bridge is illustrated in Figure 2, while the finite element model created in ABAQUS is demonstrated in Figure 3.

## 2.3 Mesh size

The accuracy of stress and strain predictions in a finite element model (FEM) is contingent on the mesh size and geometry selected. Therefore, in order to obtain an appropriate mesh refinement for the finite element model (FEM) of the historical tower, a range of mesh sizes was

applied, and analyses were carried out under multiple scenarios. It is evident that augmenting the quantity of nodes in a finite element model has the potential to enhance the precision of results. However, it is imperative to acknowledge that this augmentation can concomitantly result in a substantial augmentation in computation time. The three-dimensional representation of the tower was initially developed using Solidworks and subsequently transferred into Abaqus for further processing. In the Abaqus-based finite element model (FEM), a total of 27,985 nodes and 15,235 C3D10 tetrahedral elements were implemented. The C3D10 element is a ten-node tetrahedral solid that is frequently employed for general-purpose simulations. Prior to the execution of the analysis, the most suitable mesh size was selected.

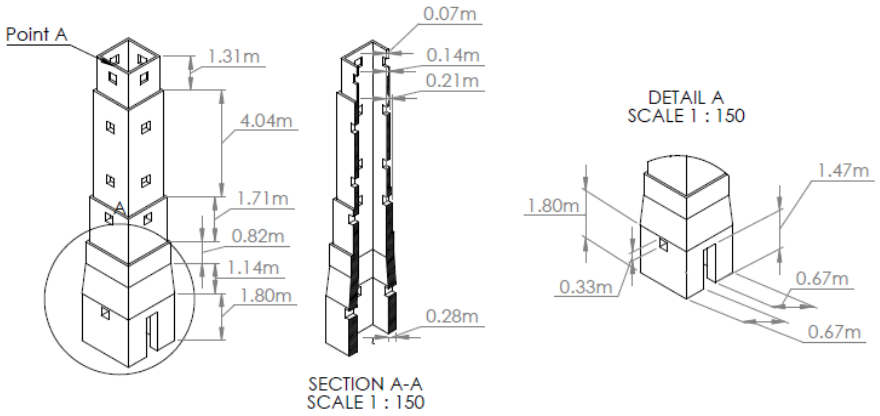


*Figure 2: Geometry of the Yozgat clock tower*

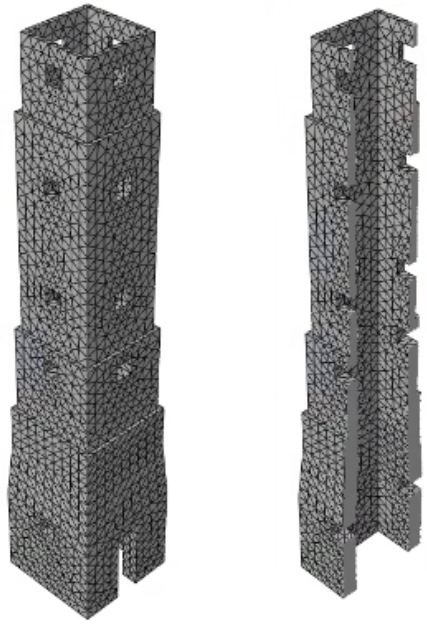

*Figure 3: Three dimensional finite element model of the tower*

A series of simulations were conducted, with mesh sizes ranging from 1 metre to 0.21 metres. Following a thorough analysis of the available results, it was determined that the optimal mesh size is 0.26 metres. The detailed outcomes of the analysis are summarised in Table 1.

Convergence analysis was performed using the values in Table 1, and the graph in Figure 4 was obtained.

*Table 1: Number of elements and mode 1 frequency values*

| Number of elements | First frequency values (Hz) |
|---|---|
| 957 | 5.8220 |
| 1282 | 5.6986 |
| 2276 | 5.6704 |
| 4882 | 5.6585 |
| 8386 | 5.6512 |
| 11,051 | 5.6490 |
| 15,235 | 5.6398 |
| 17,762 | 5.6393 |
| 23,648 | 5.6376 |

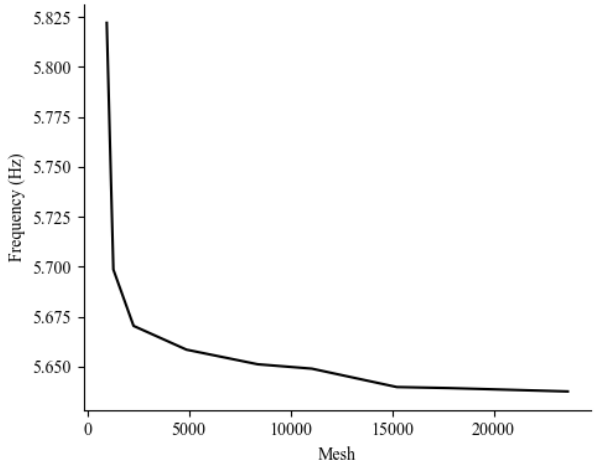


*Figure 4: Mesh convergence graph*

## 2.4 Material properties

In view of the challenges encountered in the determination of material properties for these structures, a comprehensive review of extant literature was undertaken to establish the relevant material properties [35, 36, 37]. As illustrated in Table 2, the primary physical and mechanical characteristics of the bridge material under consideration in this investigation are presented.

*Table 2: Main material characteristic of the Yozgat Clock Tower*

| Material | Density (kg/m$^3$) | Modulus of Elasticity (MPa) | Poisson's ratio |
|---|---|---|---|
| Stone | 1900 | 4400 | 0.15 |

The Concrete Damaged Plasticity (CDP) model describes the deterioration of the material properties using the plasticity theory coupled with the damage mechanics theory. The model describes the two major types of failures exhibited by concrete, which are the tension failures

that result in the formation of cracks, as well as the compression failures that result due to the crushing effect of the material. Even though the model is mainly utilised for the simulation of the effects of dynamic loads, the model has been widely used where the material experiences repeated loads [35]. The model has both nonlinear tension and compression responses, as indicated in Figure 3, which clearly shows that the model is nonlinear when subjected to compression and tension loads [38]. Even though the Concrete Damaged Plasticity model is specifically defined for the simulation of the effects of loads on the concrete, the model can also be utilised for the simulation of loads for the masonry material as well, if the parameters are correctly defined for the material properties. As demonstrated in Figure 5, the model typically exhibits behaviour in a predictable manner when subjected to uniaxial loading conditions. The parameters necessary for defining the CDP model in this study are presented in Tables 3 and 4 [35].

The uniaxial tension and compression responses in the CDP model are characterised by damage variables that reflect the evolution of structural deterioration. In the context of tensile loading, the response of the material is characterised by a linear elastic region up to the tensile strength ($\sigma$nto). Beyond this point, microcracking initiates and the stress–strain curve enters a softening regime, as illustrated in Figure 5. In the case of compressive loading, the model captures elastic behaviour until the compressive strength ($\sigma$co) is reached. Beyond this point, the material undergoes a process of crushing, which is followed by a nonlinear softening behavior, representing progressive material failure (Figure 5).

*Table 3: CDP parameters [35]*

| Dilation angle | Eccentricity | $\sigma_{bo}$ / $\sigma_{co}$ | K | Viscosity |
|---|---|---|---|---|
| 10 | 0.1 | 1.166 | 0.666 | 0.001 |

*Table 4: Stress and strain values employed in the CDP model [35]*

| Compression | | Tension | |
|---|---|---|---|
| $\sigma_c$ (Mpa) | Plastic strain | $\sigma_t$ (Mpa) | Plastic strain |
| 2 | 0 | 0.2 | 0 |
| 2 | 0.0015 | 0.02 | 0.0025 |
| 0.2 | 0.005 | 0.02 | 0.01 |
| Damage in compression | | Damage in tension | |
| $d_c$ | Plastic strain | $d_t$ | Plastic strain |
| 0 | 0 | 0 | 0 |
| 0.95 | 0.005 | 0.95 | 0.005 |

## 2.5 Determination of seismic parameters

A comprehensive investigation was conducted to assess the seismic response of the tower. The following methodology was employed in order to achieve this objective. Firstly, the data concerning the DD-2 earthquake ground motion level, as established in TBDY 2018 [39], were retrieved from the Turkey Earthquake Hazard Map interactive web application [40]. The retrieval process was informed by the characteristics of the region in which the tower is situated. The earthquake data obtained are presented in Table 5. The acceleration records of the earthquakes

that were utilised for seismic analysis were obtained from the AFAD [41], and a matching process was performed for the region in which the seismic activity was observed, specifically the area encompassing the Yozgat Clock Tower, with the assistance of Seismo Match software.

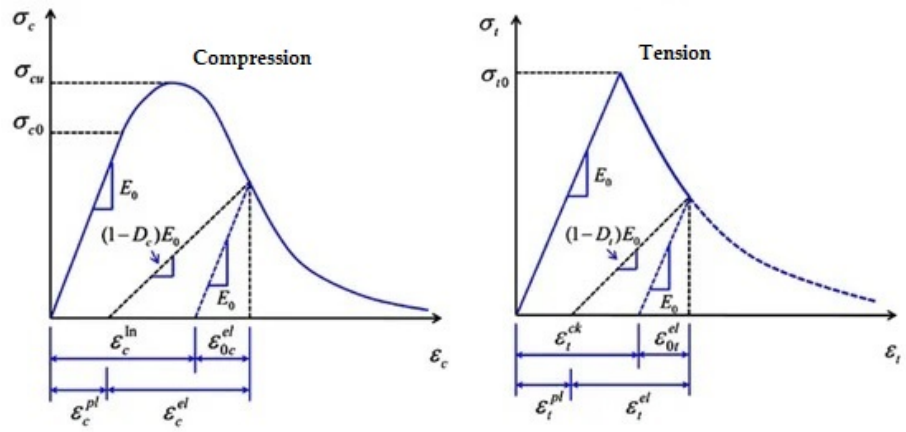


*Figure 5: Concrete damage plasticity stress-strain diagrams*

*Table 5: Earthquake data [41]*

| Earthquake ground motion level | Local ground class | Ss | $S_1$ |
|---|---|---|---|
| DD2 | ZC | 0.298 | 0.124 |

Acceleration records from the 2023 Pazarcık earthquake were utilised in time history analyses (Table 6). During the selection process for the acceleration record, meticulous attention was paid to the necessity of ensuring that the Vs30 (average shear wave velocity at 30 metres from the surface) values of the recording station and the tower structure location were in close proximity to each other. This was done in order to enhance the accuracy of the analyses and their suitability for the local soil conditions. The seismic parameter Vs30 is of particular relevance in ground classification and the assessment of ground motion amplification effects.

*Table 6: The earthquake used in time history analysis [41]*

| Earthquake | Date | Station Code | Mw | Original | | Matched | |
|---|---|---|---|---|---|---|---|
| | | | | PGA (g) | PGV (cm/s) | PGA (g) | PGV (cm/s) |
| Pazarcik East-West | 06.02.2023 | 4614 | 7.7 | 2.208 | 70.17 | 0.157 | 14.68 |
| Pazarcik North-South | 06.02.2023 | 4614 | 7.7 | 1.992 | 92.41 | 0.175 | 14.37 |

The Vs30 value for the tower was determined to be 491.35 m/s, while for the selected station (4614) this figure was found to be 474.47 m/s. It is evident that these two values exhibit only a limited disparity, with both reflecting analogous ground conditions. The observation that the Vs30 values are in close proximity suggests that the selected station exhibits considerable compatibility with the tower in terms of local ground properties. Consequently, the utilisation of ground vibrations from this station in time history analyses ensured an accurate representation of the interaction between the soil and the structure, thereby enhancing the reliability of the model.

The scaled response spectra obtained from the Seismo Match software are shown in Figure 6, and the matched and original acceleration records are shown in Figure 7.

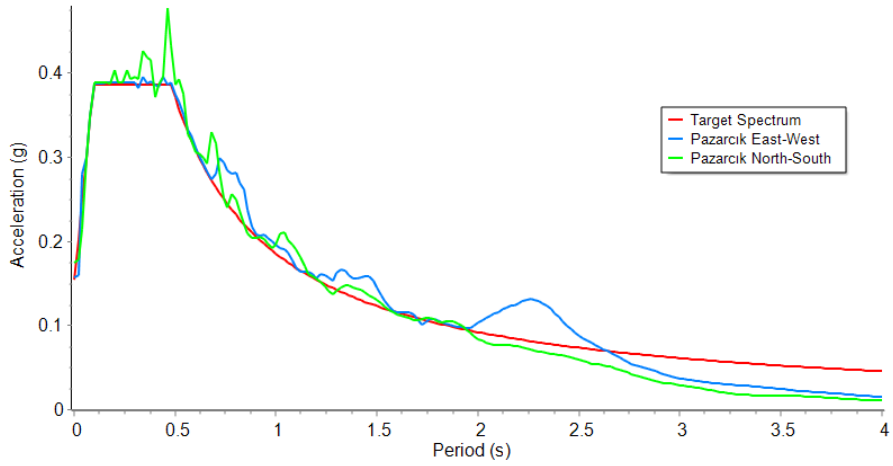


*Figure 6: Matched response spectrum*

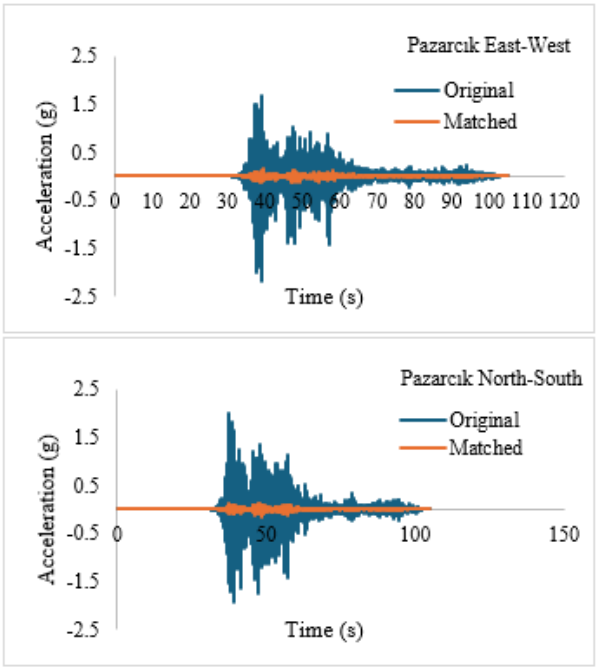


*Figure 7: Matched and original acceleration records*

# 3 Results and discussion

## 3.1 Modal analysis

Mode shapes are of particular significance in the study of the general behaviour of the towers. In the course of performing modal analysis, solutions were obtained for a total of 12 modes. The mass participation ratios for the initial and concluding five modes are displayed in Table 7. The initial five mode shapes that were obtained as a consequence of the modal analysis are presented in Figure 8.

As indicated by the results of the modal analysis, the behaviour of the structure under investigation was found to be characterised by lateral bending in the first four modes. The initial two modes are representative of the fundamental bending modes in the x and y directions,

respectively. The structure manifests unidirectional oscillatory motion in these modes. It was observed that more complex bending patterns involving multiple nodes emerged in the third and fourth modes, indicating that these modes represent higher-order lateral bending modes. The fifth mode demonstrates a distinctive rotational movement around the structure axis, thereby illustrating torsional behaviour. These results show the directionally variable nature of structure dynamic properties, with the torsional mode being effective at a higher level of frequency.

*Table 7: Mass participation ratios*

| Mode | Frequency (Hz) | Mass participation ratio | | |
|---|---|---|---|---|
| | | X direction | Y direction | Z direction |
| 1 | 5.64 | 0.00 | 44.96 | 0.00 |
| 2 | 5.70 | 45.70 | 44.96 | 0.00 |
| 3 | 18.27 | 75.06 | 44.96 | 0.00 |
| 4 | 19.21 | 75.06 | 72.30 | 0.02 |
| 5 | 22.28 | 75.91 | 72.30 | 0.02 |
| 96 | 186.83 | 94.41 | 94.46 | 89.99 |
| 97 | 186.95 | 94.43 | 94.46 | 89.99 |
| 98 | 189.76 | 94.43 | 94.46 | 90.00 |
| 99 | 189.96 | 94.43 | 94.46 | 90.99 |
| 100 | 191.00 | 94.43 | 94.50 | 90.99 |

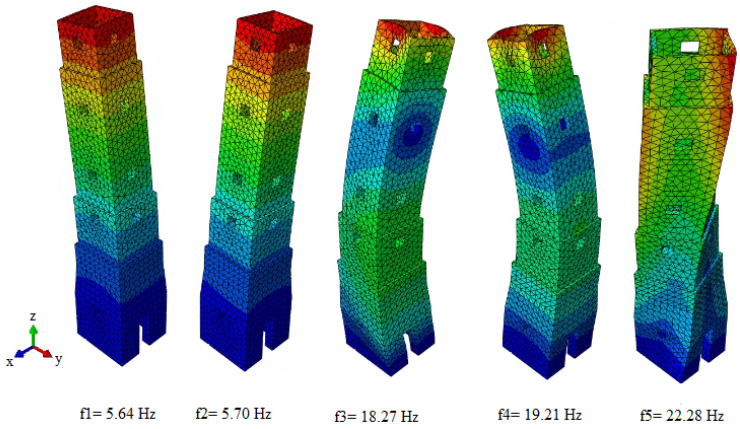


*Figure 8: Modal analysis results*

In the time history analysis, the values of the viscous damping coefficients were determined through the use of the Rayleigh damping method. Through this method, the values of the $\alpha$ (mass) coefficient and the $\beta$ (stiffness) coefficient of damping were calculated based on the first natural frequency of the structure and another frequency where the total modal mass participation ratio exceeded 90%, with the target damping ratio of 5%. This method provided effective damping over a broad range of frequencies in relation to the low-frequency rigid-body dynamics and the high-frequency vibration components. Consequently, the effects of artificial damping were kept to a minimum, and a physically consistent and balanced damping behaviour was achieved. The Rayleigh damping coefficients were calculated and then applied uniformly throughout all time history simulations. This ensured an accurate representation of the structural dynamic response.

The following Table 8 shows the formulae proposed in the existing literature for the prediction of the fundamental period of masonry towers, along with the frequency values determined by these formulae.

*Table 8: Frequencies calculated according to formulas suggested in the literature*

| Reference | Suggested Formula | Calculated Period, f (Hz) | f1 / f (5.64 Hz) |
|---|---|---|---|
| NTC [42] | $f(H) = \frac{1}{0.05\ H^{3/4}}$ | 2.880 | 2.0 |
| Shakya et. al. [43] | $f(H) = \frac{1}{0.0151\ H^{1.08}}$ | 4.065 | 1.4 |
| Ranieri and Fabbrocino [44] | $f(H) = \frac{1}{0.01137\ H^{1.138}}$ | 4.647 | 1.2 |
| Faccio et. al. [45] | $f(H) = \frac{1}{0.0187\ H}$ | 4.036 | 1.4 |
| Testa et al. [46] | $f(H) = 42.12\ \frac{1}{H^{0.893}}$ | 4.191 | 1.7 |
| Diaferio et. al. [47] | $f(H) = 28.35\ \frac{1}{H^{0.83}}$ | 3.320 | 1.3 |
| | $f(H) = 135.343\ \frac{1}{H^{1.32}}$ | 4.468 | 1.3 |

The structure's first natural frequency, 5.64 Hz, was then compared with frequency values obtained using empirical formulas proposed by various researchers in the literature. The results of this comparison are presented in Table 8. Theoretical frequencies, calculated based on the structure's height, range from 2.88 Hz to 4.65 Hz. These values are lower than the frequency of the existing structure, and the f1/f ratio varies between 1.2 and 2.0. The lowest frequency value was obtained by the NTC formula, while the Ranieri and Fabbrocino formula provided the closest estimate to the structure's frequency [42, 44]. It has been demonstrated that alternative formulations underestimate the frequency of the structure in question by approximately 30–50%. The observed discrepancies can be attributed to the utilisation of solely the structure's height as an input parameter in these empirical formulas. This approach overlooks the potential impact of other influential parameters, including geometric ratios, material properties, and stiffness, resulting in deviations in the estimated values. Consequently, it can be posited that the accuracy of empirical models for such structures is limited, and multi-parameter approaches are required for more reliable predictions.

## 3.2 Time history analysis

Nonlinear time history analysis was performed using earthquake acceleration records that had been matched and which are given in Table 6 on the Yozgat Clock Tower.

As illustrated in Figure 9, the analysis of time history reveals the occurrence of the most significant base shear forces in the horizontal direction.

Time-history analyses of the Pazarcık earthquake record yielded maximum base shear forces of approximately 94.39 kN and 93.98 kN in the X and Y directions, respectively. When these values are compared to the total mass of the structure, which is approximately 535 kN, it can be deduced that the horizontal base shear ratios are approximately 17.7% in both directions. The findings suggest that the tower exhibits analogous base shears in the horizontal direction during seismic events, with its dynamic response primarily governed by horizontal vibration modes.

As illustrated in Figure 10, the maximum and minimum principal stress distributions were obtained from time-history analyses performed on the tower. The maximum principal stress value of 1.829 MPa and the minimum principal stress value of -5.748 MPa both occurred primarily at the base of the tower. The positive principal stresses correspond to tension, while the negative principal stresses correspond to compression. This is in line with what would be

expected in a masonry tower when subjected to earthquake loading. Therefore, there was high compressive and tensile stress developed at the tower's foundation due to the earthquake.

Figure 11 tension damage contours, compressive damage contours, PEEQT, PEEQ, & PEEQC contour. The Damaget & Damagec represent the reduction in the element due to tension stresses, and Damagec shows damage developed owing to compressive stresses in each element. The PEEQT, PEEQ, and PEEQC contour plots, provided in Figure 12, represent the measure showing plastic zones developed by earthquake forces acting on the tower.

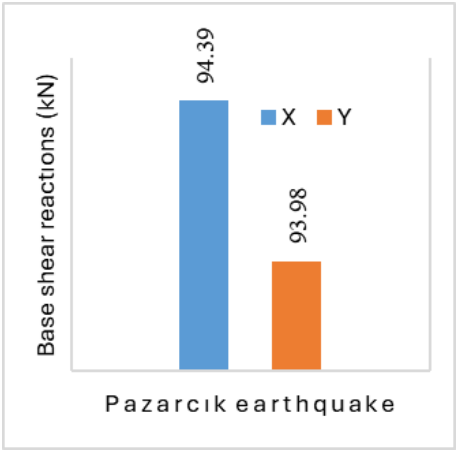


*Figure 9: The largest horizontal base shear forces*

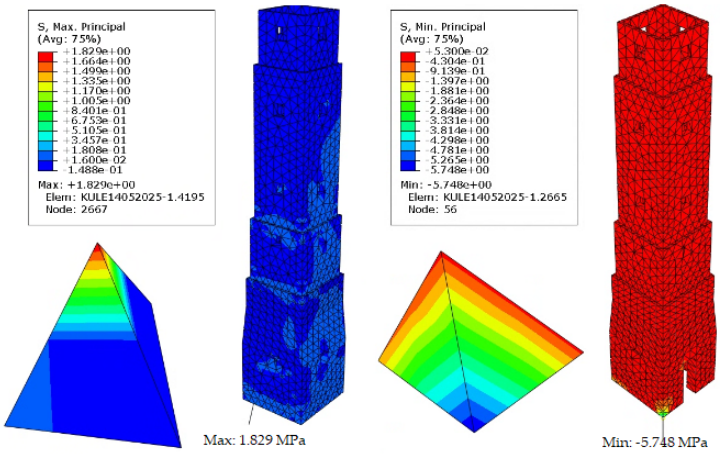


*Figure 10: Maximum and minimum principal stress contours*

As can be seen from the damage distribution results produced through time history analysis, the structure reacts in a similar manner to compression damage (DAMAGEC) as well as tension damage (DAMAGET). From the analysis results, it can be noted that the damage in the form of compression as well as tension is mainly concentrated at the base tower position with negligible damage zones in the remaining tower section. The pattern of compression damage distribution indicates that crushing damage is the major phenomenon at the tower base position, and the stresses at these locations are close to the material's load-carrying capacity. Additionally, the tension damage is localized at the tower base position, which indicates that the processes responsible for the generation as well as opening of cracks in the material started at these zones as a result of seismic action.

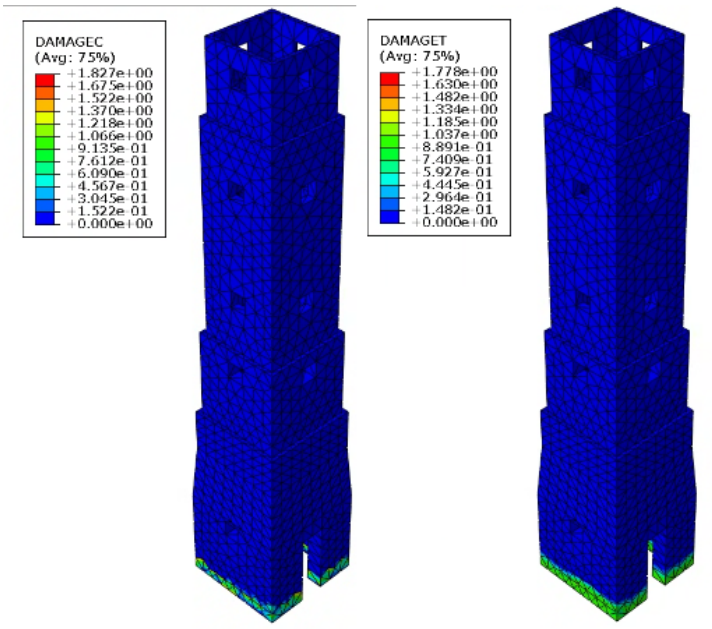


*Figure 11: Compressive and tensile damage contours*

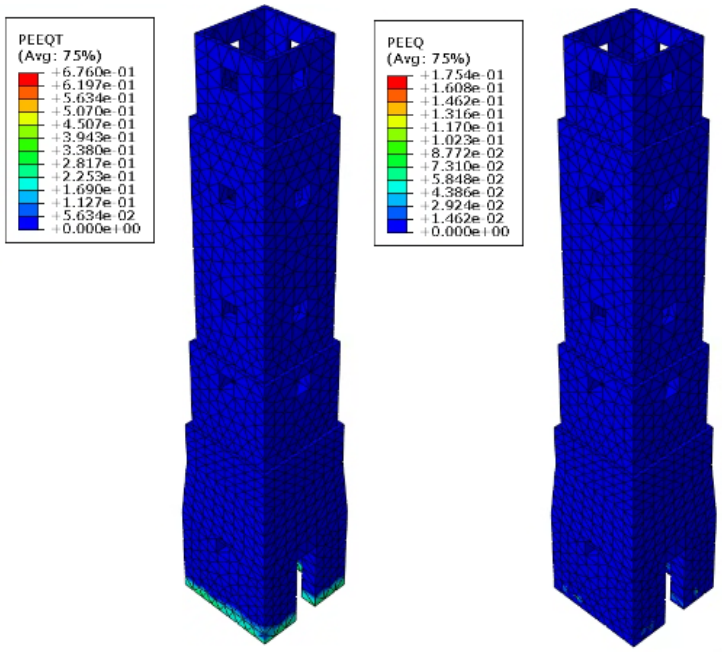


*Figure 12: PEEQT and PEEQ contours*

The PEEQT and PEEQ distribution diagrams in Figure 12 above indicate areas where plastic deformation has occurred due to the effect of earthquakes. The results are an indication that plastic deformation and, consequently, plastic deformation capability is highly concentrated at the base of the tower. PEEQT values indicate high plastic deformations, represented by red and orange hues around the base, and the values decrease rapidly towards the top, remaining within the elastic limits. Similarly, the PEEQ distribution, which represents cumulative plastic deformation, confirms that energy is dissipated primarily at the base sections, and that the upper sections of the structure exhibit rigid mass behavior under earthquake loads.

A comprehensive review of the extant literature clearly demonstrates that damage in the seismic response of masonry towers is predominantly concentrated in the base regions. Casolo et al. performed nonlinear time-history analyses under various soil conditions and stated that damage resulting from earthquake impact is mainly localised at the tower base, while the upper sections demonstrate predominantly rigid mass movement [48]. In a similar study, Valente determined that, in low- and moderate-magnitude earthquake inputs, the initial cracks predominantly form at the base and around openings [49]. As the PGA level accentuates, the damage then propagates upwards. In their study, the seismic vulnerability of masonry towers was assessed by Bartoli et al., acknowledging that the deformation and damage of the structure occur mainly at the base level, while the damage is limited to the top part of the tower [50]. Accordingly, Porcu et al. noticed that the tensile damage of masonry towers during seismic action is mainly localized at the base, confirming the predominant role of the area in the seismic vulnerability of the structure [51]. In addition, Valente and Milani have reported that the tensile damage distribution of historical masonry towers, as determined by nonlinear dynamic simulations, is predominantly concentrated at the base, with limited damage observed in the upper parts [52].

In order to undertake a quantitative assessment of the damage distribution of the structure in question in the context of seismic activity, the number of elements that have exceeded the 0.95 damage threshold was determined. The values were calculated separately for both compressive and tensile damage, and are summarised in Table 9.

*Table 9: Number of finite elements exceeding the 0.95 damage threshold*

| Parameter | Number of elements exceeded 0.95 |
|---|---|
| DAMAGEC | 154 |
| DAMAGET | 1376 |

As illustrated in Table 9, the number of elements that exceed the 0.95 threshold is 154 for compression damage (DAMAGEC) and 1,376 for tension damage (DAMAGET). This finding indicates that tension damage may manifest over a more extensive area and to a greater extent than compression damage in the structure. In accordance with the typical behaviour of masonry structures, cracking and tension damage are predominant in the aftermath of seismic events, while compression damage is concentrated in more limited areas.. Such a result shows that the seismic response of the structure, especially its tensile strength, plays a crucial role, and the focus should be on controlling the crack in possible retrofitting measures.

# 4 Conclusion

In this research, the dynamic behavior of the historical clock tower in Yozgat was investigated. In order to achieve this, a finite element model was created in ABAQUS with high accuracy. The model was subjected to modal and nonlinear time history analyses, with the Concrete Damaged Plasticity model being used. The most significant result obtained can be seen below.

Based on the modal analysis, the first natural frequency of the tower was found to be 5.64 Hz. For comparison, the calculated frequencies using empirical formulas in the literature were found to be fairly close to 5.64 Hz, but the formulas in which the parameter is only the structure's height tended to give a slightly lower estimate of the frequency.

The results of the nonlinear time history analyses indicated that both tensile and compressive damages occurred mostly in the base region of the tower, while the seismic response of the

structure was dominated by the damage in the base region. It was also noted that tensile damage was more scattered compared to the compressive damage, and this suggested that the mechanics of cracking was the dominant feature in the seismic response of the tower. Moreover, the base regions of the structure were predominantly prone to both plastic and permanent deformation, while the top regions were mostly resistant to rigid mass movement, and this limited the damage to these regions. These findings agree with existing research that suggests the base region of the structure is usually the dominant region in determining the vulnerability of the structure during seismic responses. Additionally, the base shear forces calculated in the horizontal directions were comparable, and these forces represented about 17.7% of the total weight of the structure.

Analysis of the study results shows that the seismic response of the tower is mainly controlled by the brittle response of its foundation. Hence, the measures for upgrading the seismic-resistant performance of the structure should primarily be focused on its foundation level. Additionally, future research works might be conducted on seismic response analysis of this structure, taking into consideration both soil-structure interaction and probabilistic seismic analysis.

# Supplementary materials

Supplementary materials comprise the comprehensive Abaqus finite element model files, the thorough Concrete Damaged Plasticity (CDP) material parameters, the processed ground motion records utilised in the nonlinear analyses and the high-resolution figures and visualisations that provide support and complement the findings presented in the manuscript.

# Acknowlegdments

The authors would like to acknowledge all individuals whose support and contributions have facilitated the completion of this research.

# Conflict of interest

The authors declare no conflict of interest.

# References

[1] Milani, G., Casolo, S., Naliato, A., & Tralli, A. (2012). Seismic assessment of a medieval masonry tower in Northern Italy by limit, nonlinear static, and full dynamic analyses. *International Journal of Architectural Heritage, 6*(5), 489-524.

[2] Carmona, J. R., Porras, R., Yu, R. C., & Ruiz, G. (2013). A fracture mechanics model to describe the buckling behavior of lightly reinforced concrete columns. *Engineering Structures, 49*, 588-599.

[3] Kumar, A., & Pallav, K. (2024). Finite element analysis of a 108-year-old unreinforced brick masonry tower following the 2015 Nepal earthquakes. *Asian Journal of Civil Engineering, 25*(2), 2175-2188.

[4] Onat, O., Toy, A. T., & Özdemir, E. (2023). Block masonry equation-based model updating of a masonry minaret and seismic performance evaluation. *Journal of Civil Structural Health Monitoring, 13*(6), 1221-1241.

[5] Romero-Sánchez, E., Morales-Esteban, A., Bento, R., & Navarro-Casas, J. (2023). Numerical modelling for the seismic assessment of complex masonry heritage buildings: the case study of the Giralda tower. *Bulletin of Earthquake Engineering, 21*(9), 4669-4701.

[6] Peña, F., Lourenço, P. B., Mendes, N., & Oliveira, D. V. (2010). Numerical models for the seismic assessment of an old masonry tower. *Engineering Structures, 32*(5), 1466-1478.

[7] Çaktı, E., Saygılı, Ö., Lemos, J. V., & Oliveira, C. S. (2020). Nonlinear dynamic response of stone masonry minarets under harmonic excitation. *Bulletin of Earthquake Engineering, 18*(10), 4813-4838.

[8] Romero-Sánchez, E., Requena-Garcia-Cruz, M. V., & Morales-Esteban, A. (2025, April). Seismic performance of a masonry tower under non-linear methods. In *Structures* (Vol. 74, p. 108458). Elsevier.

[9] Chisari, C., Zizi, M., Lavino, A., Freda, S., & De Matteis, G. (2024). Operational Modal Analysis and Safety Assessment of a Historical Masonry Bell Tower. *Applied Sciences, 14*(22), 10604.

[10] Romero-Sanchez, E., Requena-Garcia-Cruz, M. V., & Morales-Esteban, A. (2024). Impact of the soil-foundation-structure interaction in the seismic behaviour of a heritage masonry tower: The Giralda of Seville. *Engineering Failure Analysis, 163*, 108580.

[11] Najafgholipour, M. A., Hamidian, Z., Darvishi, H., & Gardoni, P. (2025). The failure assessment of historical masonry towers subjected to near-field and far-field ground motions. *Engineering Failure Analysis,* 109856.

[12] Çakıroğlu, M. A., Evci, P. U., Sever, A. E., & Kaplan, A. N. (2025). The Effects of Shotcrete Strengthening on the Seismic Vulnerability of an Existing Masonry Building Damaged in the 6th of February Kahramanmaraş Türkiye Earthquakes. *Journal of Earthquake and Tsunami, 19*(6), 2550017.

[13] Uysal, N., & Evci, P. U. (2025). Investigation of the dynamic behavior of a registered masonry building in Turkey and strengthening suggestions by CFRP. *Journal of Earthquake and Tsunami, 19*(4), 2450012.

[14] Valente, M., & Milani, G. (2016). Non-linear dynamic and static analyses on eight historical masonry towers in the North-East of Italy. *Engineering Structures, 114*, 241-270.

[15] Minghini, F., Bertolesi, E., Del Grosso, A., Milani, G., & Tralli, A. (2016). Modal pushover and response history analyses of a masonry chimney before and after shortening. *Engineering Structures, 110*, 307-324.

[16] Acito, M., Bocciarelli, M., Chesi, C., & Milani, G. (2014). Collapse of the clock tower in Finale Emilia after the May 2012 Emilia Romagna earthquake sequence: Numerical insight. *Engineering Structures, 72*, 70-91.

[17] De Silva, F. (2020). Influence of soil-structure interaction on the site-specific seismic demand to masonry towers. *Soil Dynamics and Earthquake Engineering, 131*, 106023.

[18] Maraş, M. M., Özmen, A., Sayın, E., & Ayaz, Y. (2022). Seismic assessment of the historical Sütlü Minaret Mosque. *Periodica Polytechnica Civil Engineering, 66*(2), 445-459.

[19] Scamardo, M., Zucca, M., Crespi, P., Longarini, N., & Cattaneo, S. (2022). Seismic vulnerability evaluation of a historical masonry tower: Comparison between different approaches. *Applied Sciences, 12*(21), 11254.

[20] Najafgholipour, M. A., Darvishi, H., & Maheri, M. R. (2021). The influence of the frequency content of ground motion on the nonlinear dynamic response and seismic vulnerability of historical masonry towers. *Bulletin of Earthquake Engineering, 19*(7), 2919-2940.

[21] Magrinelli, E., Acito, M., & Bocciarelli, M. (2021). Numerical insight on the interaction effects of a confined masonry tower. *Engineering Structures, 237*, 112195.

[22] Khider, T. A., & Al-Baghdadi, H. A. (2020). Dynamic response of historical masonry minaret under seismic Excitation. *Civil Engineering Journal, 6*(1), 142-155.

[23] Ferrante, A., Clementi, F., & Milani, G. (2020). Advanced numerical analyses by the Non-Smooth Contact Dynamics method of an ancient masonry bell tower. *Mathematical Methods in the Applied Sciences, 43*(13), 7706-7725.

[24] Pekgökgöz, R., Avcıl, F., Baltacı, G., & Gürel, A. (2022). Yığma Bir Seyir Kulesinin Dinamik Analizi. *Avrupa Bilim ve Teknoloji Dergisi,* (35), 455-463.

[25] Demir, C., Comert, M., Inci, P., Dusak, S., & Ilki, A. (2023). Seismic retrofitting of the 19th century Hirka-i Serif Mosque using textile reinforced mortar. *International Journal of Architectural Heritage, 17*(8), 1364-1387.

[26] Kouris, E. G., Kouris, L. A. S., Konstantinidis, A. A., Karayannis, C. G., & Aifantis, E. C. (2021). Assessment and fragility of Byzantine unreinforced masonry towers. *Infrastructures, 6*(3), 40.

[27] Kılıç, İ., Bozdoğan, K. B., Aydın, S., Gök, S. G., & Gündoğan, S. (2019). Kule tipi yapıların dinamik davranışının belirlenmesi: kırklareli hızırbey camii minaresi. *Politeknik Dergisi, 23*(1), 19-26.

[28] Trešnjo, F., Humo, M., Casarin, F., & Ademović, N. (2023). Experimental investigations and seismic assessment of a historical stone minaret in Mostar. *Buildings, 13*(2), 536.

[29] Anadut, H. O. (2016). *Investigation of the Dynamic Behavior of Historical Structures*. Master's Thesis, 2016.

[30] Milani, G., & Valente, M. (2015). Failure analysis of seven masonry churches severely damaged during the 2012 Emilia-Romagna (Italy) earthquake: Non-linear dynamic analyses vs conventional static approaches. *Engineering Failure Analysis, 54*, 13-56.

[31] Sarhosis, V., De Santis, S., & de Felice, G. (2016). A review of experimental investigations and assessment methods for masonry arch bridges. *Structure and Infrastructure Engineering, 12*(11), 1439-1464.

[32] Fanning, P. J., & Boothby, T. E. (2001). Three-dimensional modelling and full-scale testing of stone arch bridges. *Computers & Structures, 79*(29-30), 2645-2662.

[33] Lourenço, P. B. (2002). Computations on historic masonry structures. *Progress in Structural Engineering and Materials, 4*(3), 301-319.

[34] Gönen, S., & Soyöz, S. (2021). Seismic analysis of a masonry arch bridge using multiple methodologies. *Engineering Structures, 226*, 111354.

[35] Hökelekli, E., & Al-Helwani, A. (2020). Effect of soil properties on the seismic damage assessment of historical masonry minaret–soil interaction systems. *The Structural Design of Tall and Special Buildings, 29*(2), e1694.

[36] Altıok, T. Y. (2019). *Tarihi Minarelerin Dinamik Özelliklerinin Deneysel Ve Nümerik Yöntemler Ile Araştırılması*. Master's dissertation, Manisa Celal Bayar University, Manisa.

[37] Şeker, S., & Şahin, H. (2022). Evaluation of the Seismic Behavior of the Historic Clandras Bridge. *Usak University Journal of Engineering Sciences, 5*(1), 1-12.

[38] Öztürk, H. (2026). *Betonarme Kısa Kirişlerde Kesme Dayanımı*. PhD Thesis, 2016.

[39] ÖZTÜRK, M. (2018). 2018 Türkiye bina deprem yönetmeliği ve türkiye deprem tehlike haritasi ile ilgili iç anadolu bölgesi bazinda bir değerlendirme. *Selcuk University Journal of Engineering Sciences, 17*(2), 31-42.

[40] Erkin, Ö., Yenigün, S., Gümüş, C., Coşğun, M., & Aslan, G. (2024). Afet ve acil durum yönetimi başkanlığı (AFAD) afet eğitimlerinin hemşirelik öğrencilerinin afet yönetimi algısına etkisi. *Afet ve Risk Dergisi, 7*(1), 47-61.

[41] AFAD. Earthquake Service. `https://tadas.afad.gov.tr` (accessed 27 Apr 2025).

[42] NTC. *Norme Tecniche per le Costruzioni*. D.M. 14/01/2008.

[43] Shakya, M., Varum, H., Vicente, R., & Costa, A. (2016). Empirical formulation for estimating the fundamental frequency of slender masonry structures. *International Journal of Architectural Heritage, 10*(1), 55-66.

[44] Rainieri, C., & Fabbrocino, G. (2011, September). The elastic period of masonry towers: empirical correlations for prediction. In *XIV National Congress on Earthquake Engineering in Italy, Bari* (pp. 18–22).

[45] Faccio, P., Podestà, S., & Saetta, A. (2010). VENEZIA, IL CAMPANILE DELLA CHIESA DI SANT'ANTONIN-Torri, campanili ed altre strutture a prevalente sviluppo verticale. In *Linee Guida per La Valutazione E Riduzione Del Rischio Sismico Del Patrimonio Culturale–allineamento Alle Nuove Norme Tecniche per Le Costruzioni* (pp. 292-323). Gangemi.

[46] Testa, F., Barontini, A., & Lourenço, P. B. (2024). Development and validation of empirical formulations for predicting the frequency of historic masonry towers. *International Journal of Architectural Heritage, 18*(7), 1164-1184.

[47] Diaferio, M., Foti, D., & Potenza, F. (2018). Prediction of the fundamental frequencies and modal shapes of historic masonry towers by empirical equations based on experimental data. *Engineering Structures, 156*, 433-442.

[48] Casolo, S., Diana, V., & Uva, G. (2017). Influence of soil deformability on the seismic response of a masonry tower. *Bulletin of Earthquake Engineering, 15*(5), 1991-2014.

[49] Valente, M. (2021). Seismic vulnerability assessment and earthquake response of slender historical masonry bell towers in South-East Lombardia. *Engineering Failure Analysis, 129*, 105656.

[50] Bartoli, G., Betti, M., Galano, L., & Zini, G. (2019). Numerical insights on the seismic risk of confined masonry towers. *Engineering Structures, 180*, 713-727.

[51] Porcu, M. C., Montis, E., & Saba, M. (2021). Role of model identification and analysis method in the seismic assessment of historical masonry towers. *Journal of Building Engineering, 43*, 103114.

[52] Valente, M., & Milani, G. (2018). Effects of geometrical features on the seismic response of historical masonry towers. *Journal of Earthquake Engineering, 22*(sup1), 2-34.